Colloids and Surfaces A: Physicochem. Eng. Aspects 426 (2013) 6–11

Contents lists available at SciVerse ScienceDirect

Colloids and Surfaces A: Physicochemical and Engineering Aspects

journal homepage: www.elsevier.com/locate/colsurfa

The layer-by-layer assembly of polyelectrolyte functionalized graphene sheets: A potential tool for biosensing

Jianbo Ma, Peng Cai, Wei Qi**, Desheng Kong, Hua Wang*

Key Laboratory of Life-Organic Analysis, Key Laboratory of Pharmaceutical Intermediates and Analysis of Natural Medicine, School of Chemistry and Chemical Engineering, Qufu Normal University, 57 Jingxuan West Road, Qufu, Shandong 273165, China

HIGHLIGHTS

- Graphene surface was functionalized with polyacrylic acid.
- The PAA–graphene was used to construct electrochemical functionalized multilayer.
- The multilayer electrode was investigated for potential use in biosensing.
- The combination of graphene and LbL technique can develop efficient biosensors.

GRAPHICAL ABSTRACT

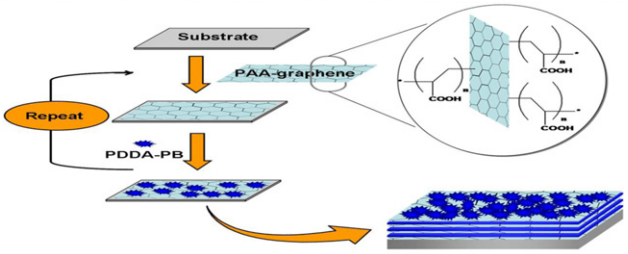

ARTICLE INFO

Article history:
Received 30 November 2012
Received in revised form 13 February 2013
Accepted 17 February 2013
Available online 1 March 2013

Keywords:
Layer-by-layer assembly
Polyacrylic acid functionalized graphene
Prussian Blue nanoparticles
Electrocatalysis

ABSTRACT

In this paper, graphene surface was functionalized with polyacrylic acid (PAA) and was used as a building block to construct electrochemically functionalized multilayer via electrostatic layer-by-layer (LbL) assembly. Prussian Blue (PB) nanoparticles protected by poly(diallyldimethylammonium chloride) (PDDA–PB) were used as an example of electroactive species for the assembly. Through electrostatic interaction, the modified-graphene (PAA–graphene) was assembled together with the positively charged PDDA–PB. Atomic force microscopy (AFM) was used to demonstrate the modification of graphene sheets and microstructure of the graphene-based multilayer. Furthermore, the multilayer (PAA–graphene/PDDA–PB)$_n$ film electrode was characterized with cyclic voltammetry for its potential use in biosensing. The electrode exhibited elctrocatalytic activity for the reduction of H_2O_2. It can be expected that this work will stimulate the development of efficient and advanced biosensing devices and the construction of new and potentially useful nanosystems.

1. Introduction

Graphene, a newly reported carbon materials with two-dimensional (2D) nanostructure, has emerged as a novel and important class of conducting materials due to its extraordinary electrical, thermal and mechanical properties since its discovery in 2004 by Geim and co-workers [1]. And graphene sheets have been extensively studied in synthesizing nanocomposites and fabricating various microelectrical devices, such as battery, field-effect transitors, ultrasensitive sensors, and electrochemical resonators [2–5]. Graphene has also great promise in electrochemical sensing and biosensing. Graphene-based electrodes have been reported to show excellent electroactivity for H_2O_2, O_2, NADH and other important electoactive species [6–10]. However, graphene sheets are very hydrophobic and form agglomerates easily and inevitably in aqueous solutions in the absence of dispersing reagents as a result of strong stacking and Van der Waals interactions. Thus, some methods have been developed to stabilize graphene sheets, either by covalent or noncovalent modification by aromatic molecules, surfactants and polymers [11–15]. As recently reported by Ye and co-workers [16], a stable and homogeneous graphene sheet dispersion could be prepared via an exfoliation/in situ reduction of graphene

* Corresponding author. Tel.: +86 537 4456306.
** Corresponding author. Tel.: +86 537 4458208; fax: +86 537 4456630.
E-mail addresses: qiwei@iccas.ac.cn (W. Qi), huawangqfnu@126.com (H. Wang).

0927-7757/$ – see front matter © 2013 Elsevier B.V. All rights reserved.
http://dx.doi.org/10.1016/j.colsurfa.2013.02.039

oxide followed by in situ living free radical polymerization of polyacrylic acid (PAA). This method prevented restacking and agglomeration of graphene sheets to form graphite through Van der Waals interaction. Its simplicity opens broad perspectives to use the charged and high dispersed graphene sheets to fabricate various composites. In this paper, graphene surface was functionalized with PAA by this method and the as-prepared PAA–graphene was used as a building block to construct electrochemically functionalized composite film.

To fabricate graphene-based composite materials, it is important to develop simple and versatile assembly methods. One method meeting the challenge to assemble graphene-based ultrathin composite films is using layer-by-layer (LbL) assembly technique introduced by Decher in 1990s [17]. The LbL assembly methods offer opportunities to prepare multilayer films with desired functions [18–23]. This strategy allows the precise control of the film thickness, composition, morphology and functionality on a nanometer scale level [24–28].

Here, by using the LbL assembly method, fabrication of multilayer ultrathin films consisting of PAA–graphene and Prussian Blue (PB) nanoparticles was described, as shown in Scheme 1. The use of PB nanostructures for the creation of the electrochemical devices is an extremely promising prospect. PB is known to be a superior electrocatalyst in hydrogen peroxide reduction [29–31]. To improve the film-forming property, the PB nanoparticles were positively charged with poly(diallyldimethylammonium chloride) protecting (PDDA–PB) [32]. The major purpose of this work was to estimate the potential use of the as-prepared graphene-based PAA–graphene/PDDA–PB multilayer film in the field of biosensing. For that, the electrochemical characterization of the ultrathin multilayer film electrode was presented.

2. Materials and methods

2.1. Materials

Expandable graphite (EG) 8099200 (~180 μm) was purchased from Qingdao BCSM. Co., Ltd. Poly(diallyldimethylammonium chloride) (PDDA, M_w: 20,000) was purchased from Aldrich and used as received. Dimethylformamide (DMF), 98% H_2SO_4, 30% H_2O_2, and potassium permanganate ($KMnO_4$) were purchased from Shanghai Chenyun Chemical and Engineering Company. Acrylic acid (AA), $NaBH_4$, $(NH_4)_2S_2O_8$, $FeCl_2{\cdot}4H_2O$ and $K_3Fe(CN)_6$ were obtained from Tianjin Damao Chemical Company. All other reagents were of analytical grade and used without further purification.

2.2. Preparation of PAA–graphene sheets and PDDA–PB nanoparticles

Expandable graphite oxide was obtained based on Hummers' method [16,33]. The obtained graphite oxide (30 mg) was first suspended in DMF/water (9:1), followed by stirring and ultrasonication for 30 min. Then 0.0248 g of $NaBH_4$ was added to the mixture. The mixture was heated in an oil bath at 80 °C for 4 h, and reduced graphene oxide (rGO) was obtained. Acrylic acid (10 g) and water were added to the flask. After stirring for 30 min, the solution was purged under dry nitrogen for 30 min to remove oxygen, followed by addition of $(NH_4)_2S_2O_8$ (100 mg dissolved in 80 mL of water). The flask was placed in a thermostated oil bath at 60 °C under stirring and sonication. After 48 h the mixture was cooled to room temperature, diluted with water, bath sonicated for 1 h, and then centrifuged. The as-prepared graphene and PAA–graphene were characterized by atomic force microscopy (AFM) and Fourier transform infrared spectroscopy (FTIR). Tapping-mode AFM imaging was performed on a Digital Instruments multimode microscope controlled by Nanoscope IIIa apparatus (Digital Instruments, Santa Barbara, CA). FTIR spectra were recorded on a NEXUS 470 spectrometer (Nicolet, USA).

PDDA protective PB nanoparticles were prepared according to a previously published procedure [29,32]. Briefly, 10 mL of a 0.01 mol L^{-1} $K_3[Fe(CN)_6]$ solution was slowly added to 10 mL of a 0.01 mol L^{-1} $FeCl_2{\cdot}4H_2O$ and 12.5 mmol L^{-1} PDDA solution under vigorous stirring at room temperature. The reaction mixture turned blue immediately, indicating the formation of PB nanoparticles. Residual PDDA polymer was removed by high-speed centrifugation and the complex was rinsed with water/actone (2:1, V/V) for at least

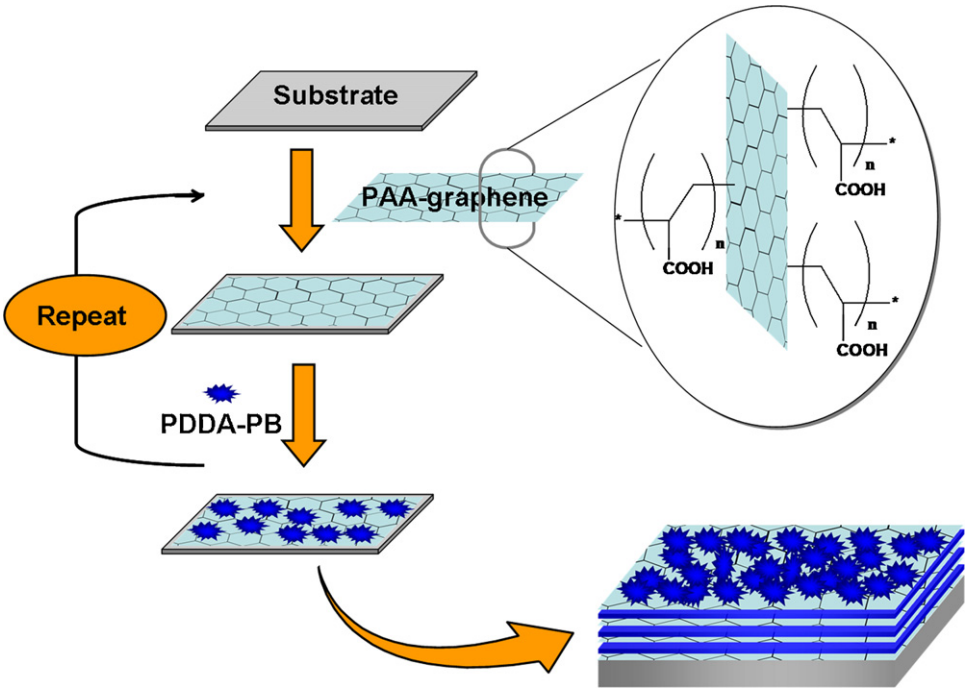

Scheme 1. Schematic representation of the assembling process of $(PAA–graphene/PDDA–PB)_n$ multilayer films. PAA–graphene: polyacrylic acid functionalized graphene, negatively charged; PDDA–PB: poly(diallyldimethylammonium chloride) protective Prussian Blue nanoparticles, positively charged.

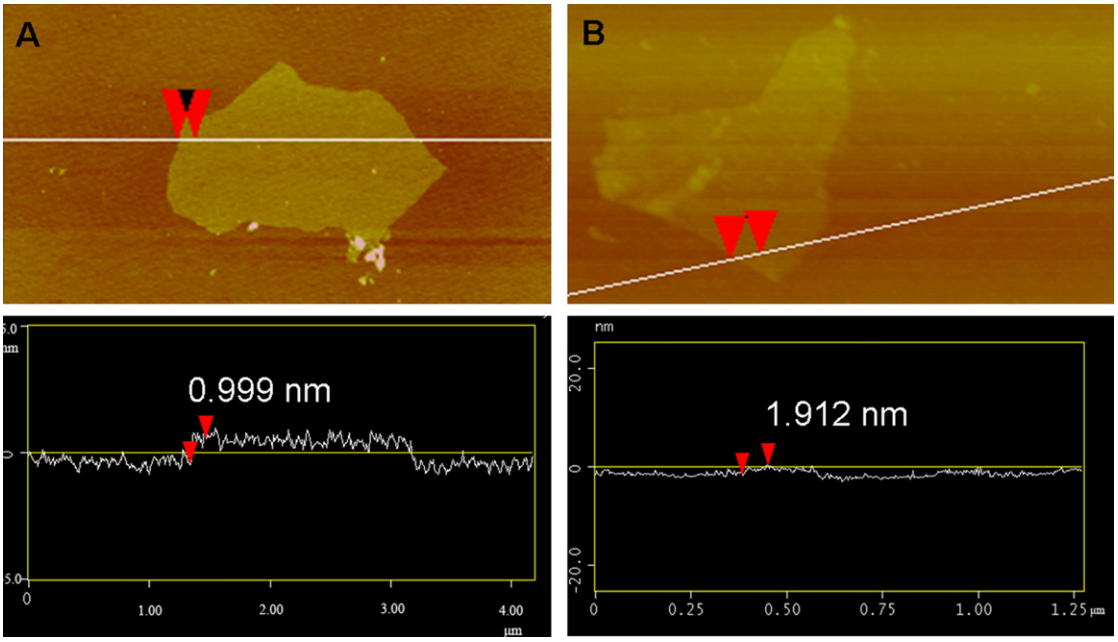

Fig. 1. AFM images and line scan of graphene (A) and PAA–graphene (B) with sheet thickness of 0.999 nm and 1.912 nm, respectively.

three times. The collected complex was redispersed in 5 mL water with mild sonicating to produce a stable PDDA–PB stock solution. The obtained PDDA–PB nanoparticles were measured by transmission electron microscopy (TEM, H-7500, Hitachi, Japan). Several drops of the PDDA–PB suspension were placed on a copper grid covered with a carbon film. Excess solutions were removed with filter paper. The resultant grid was dried in air before observation.

2.3. Layer-by-layer assembly of (PAA–graphene/PDDA–PB)$_n$ multilayer ultrathin films

Glassy carbon electrodes (GCE, 3 mm diameter) were used as the substrate to LbL assemble the graphene-based multilayer. The electrodes were polished first with emery paper and then with aqueous slurries of fine alumina powders (0.3 and 0.05 μm) on a polishing cloth and were finally cleaned with ethanol and doubly distilled water under an ultrasonic bath, each for 5 min. Multilayered films were assembled on a GCE substrate by first immersing the substrate into positively charged PDDA (1 wt% aqueous solution containing 0.5 M NaCl) for 30 min and then alternately immersing the PDDA-treated substrate into the aqueous dispersion of the negatively charged graphene nanosheets (0.25 mg/mL) and an aqueous solution of the positively charged PDDA–PB (0.1 mg/mL) for 30 min, respectively. After each immersion step, the substrate was first carefully rinsed with doubly distilled water to remove the unstably adsorbed materials and then dried with nitrogen gas.

The microstructure and growth of the multilayer were characterized by AFM and ultraviolet visible (UV–vis) spectroscopy (UV-1601, Shimadzu, Japan). (PAA–graphene/PDDA–PB)$_n$ multilayer used for AFM and UV–vis spectroscopic measurements were prepared on silicon wafers and quartz slides, respectively. The silicon wafer and quartz slide were first cleaned with piranha solution of 30% H_2O_2 and 98% H_2SO_4 (3:7 volume ratio) and then thoroughly rinsed with doubly distilled water. The assembly procedures on the silicon wafer and quartz slide were performed with the same procedures as those for the GCE substrate.

2.4. Electrochemical measurements

Electrochemical experiments were performed with a CHI 660B electrochemical analyzer (Chenhua Co., Shanghai, China). A conventional three-electrode cell was used, including a Ag/AgCl (saturated KCl) electrode as reference electrode, a platinum wire counter electrode and a modified working GE electrode.

3. Results and discussion

3.1. Characterization of PAA–graphene and PAA–graphene/PDDA–PB film

FTIR was utilized to investigate the formation of graphene oxide (GO), rGO and PAA–graphene. In the spectrum of GO (Fig. 1), the peak at 1720 is in correspondence to C=O stretching vibration. In the spectrum of PAA–graphene, the strong peak of the C=O stretching vibration can also be seen, in which peak at 3400 and 1420 are related to the stretching vibration and deformation of O—H. These results were generally consistent with the report [16], indicating the successful preparation of PAA–graphene.

AFM was used to detect the precise microstructure of graphene sheets. A section analysis revealed that the thickness of graphene oxide is 0.999 nm (Fig. 2A), and a much larger thickness of 1.912 nm was observed for PAA–graphene (Fig. 2B). This provided the

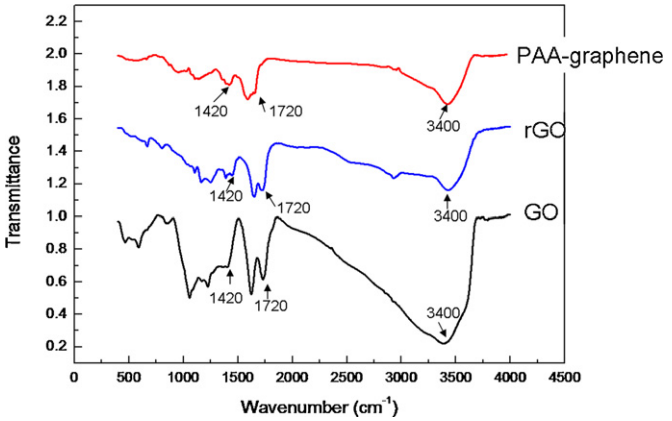

Fig. 2. FTIR spectra of graphene oxide (GO), reduced graphene oxide (rGO) and PAA–graphene.

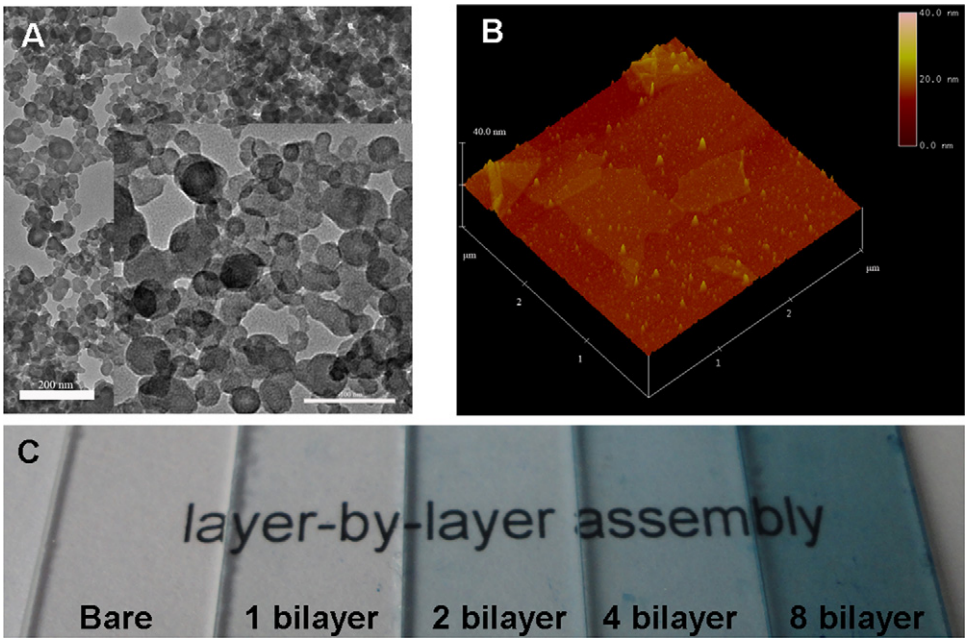

Fig. 3. (A) TEM image of PB nanoparticles. Inset is the magnified image. (B) AFM image of $(PAA–graphene/PDDA–PB)_1$ film assembled on silicon wafer. (C) Photos of $(PAA–graphene/PDDA–PB)_n$ films assembled on quartz slides with increasing bilayer numbers, $n = 1, 2, 4, 8$.

evidence for the successful attachment of PAA onto the surface of graphene sheets, consistent with previous reports [16].

PDDA–PB nanoparticle size was determined using TEM as shown in Fig. 3A. The mean average is from 20 to 40 nm. The deposited $(PAA–graphene/PDDA–PB)_1$ multilayer film was also characterized by AFM. It could be seen that PAA–graphene and PB were uniformly distributed and it showed sheet-like character. Optical images of the $(PAA–graphene/PDDA–PB)_n$ films deposited on quartz slides displayed the films had a high level of flatness and homogeneity in Fig. 3B. And the slides gradually turned dark blue indicating that thickness was increasing as deposited cycle increased.

The growth of the multilayer films prepared by the LbL method on quartz slides was followed by UV–vis absorption spectroscopy. As shown in Fig. 4, the prominent broad band at 244 nm corresponded to the absorption of graphene and the peaks at 734 nm are characteristic absorption bands of PB. The absorption increased clearly with the assembling step, indicating that PAA–graphene and PDDA–PB nanoparticles have been successfully assembled onto quartz slides.

3.2. Electrochemical characterization of $(PAA–graphene/PDDA–PB)_n$

A cyclic voltammetry (CV) study of the multilayer film electrode was performed during the assembly process. Fig. 5 showed the cyclic voltammograms of $(PAA–graphene/PDDA–PB)_n$ multilayer modified electrode with bilayer number from 1 to 4. The electrochemistry of the multilayer films showed a pair of redox peaks entered at ca. 0.2 V, corresponding to the conversion between PB and Prussian White (PW, reduced form of PB) [29,30]. Thus, the electrochemical properties of PB did not change in the multilayer assembling process. Furthermore, the redox peak height enhanced with the increase of the bilayer number, suggesting the successful deposition of PAA–graphene and PB onto GCE.

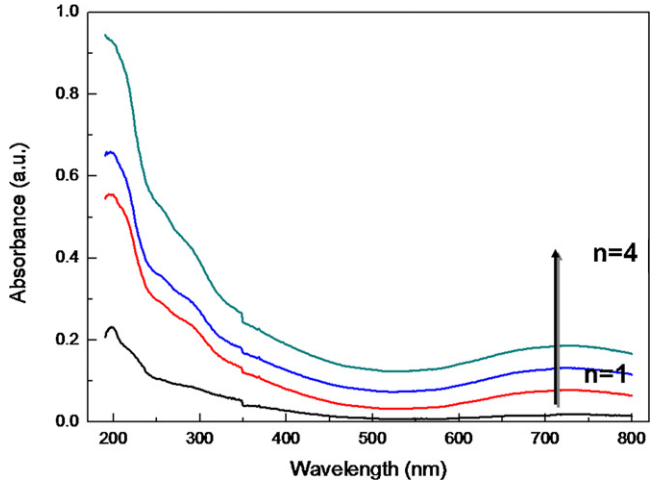

Fig. 4. UV–vis absorption spectra of $(PAA–graphene/PDDA–PB)_n$ films assembled on quartz slides, $n = 1, 2, 3, 4$.

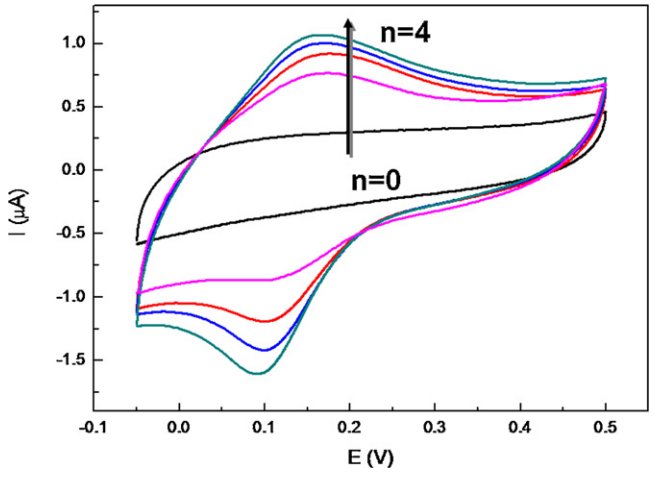

Fig. 5. Cyclic voltammograms of $(PAA–graphene/PDDA–PB)_n$ multilayer films on the glass carbon electrode in PBS of pH 7.4, containing 0.1 M KCl at a scan rate of 50 mV/s. $n = 0, 1, 2, 3, 4$.

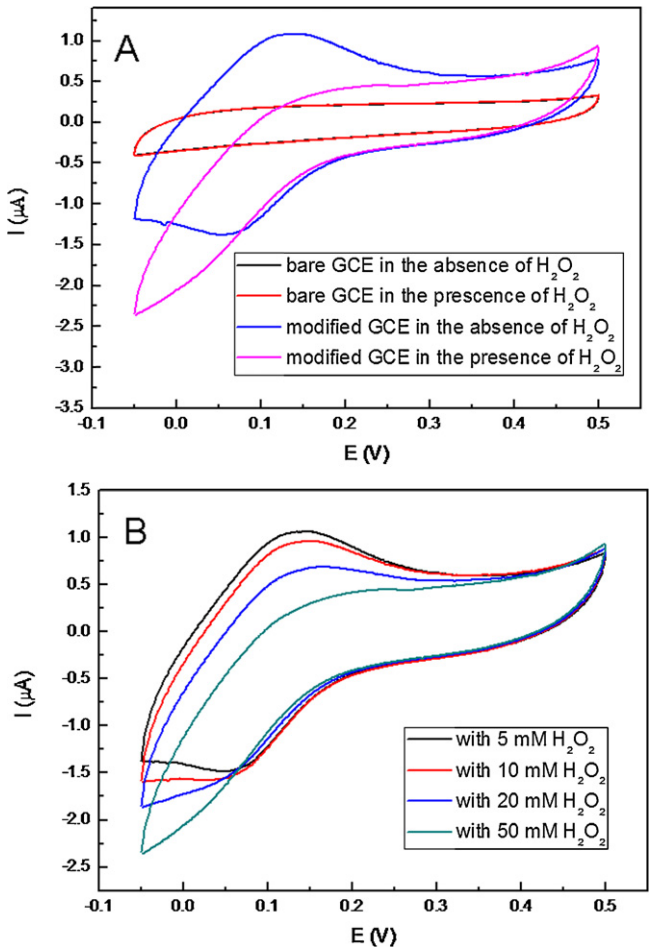

Fig. 6. (A) Cyclic voltammograms of bare GCE and $(PAA–graphene/PDDA–PB)_4$ multilayer films modified GCE in PBS of pH 7.4, containing 0.1 M KCl without and with 50 mM H_2O_2; (B) Cyclic voltammograms of $(PAA–graphene/PDDA–PB)_4$ multilayer films modified electrode in PBS of pH 7.4, containing 0.1 M KCl in the presence of H_2O_2 at a concentration ranging from 5 mM, 10 mM, 20 mM to 50 mM.

Monitoring of low levels of hydrogen peroxide is of great importance for modern medicine, environmental control, and various branches of industry. Most of importance, hydrogen peroxide is present in countless biological reactions as the main product of some oxidases and is an important parameter for monitoring of these bioporcesses [34–36]. Herein, electrocatalysis towards H_2O_2 reduction was studied to estimate the potential use in biosensing, as shown in Fig. 6. Fig. 6A showed the CV curves of bare GCE and the $(PAA–graphene/PDDA–PB)_4$ multilayer film electrode in PBS of pH 7.4, containing 0.1 M KCl in the absence and presence of 50 mM H_2O_2, respectively. It was observed that the CV curve of bare GCE did not change after 50 mM H_2O_2 was added, indicating that no response to H_2O_2 could be obtained in the range from −0.5 to 0.5 V. While in the case of the $(PAA–graphene/PDDA–PB)_4$ multilayer film electrode it exhibited a strong reduction current in the range from −0.5 to 0.5 V, indicating the electrocatalytic activity of the modified electrode towards the H_2O_2 reduction. Moreover, with varying H_2O_2 concentration from 5 mM to 50 mM, the reduction current obviously increased and the oxidation current decreased gradually (Fig. 6B). This may be ascribed to the fact that in the negative potential range, PDDA–PB (PB: $KFe(III)[Fe(II)(CN)_6]$) film can reduce to its reduction state PW (PW: $K_2Fe(II)[Fe(II)(CN)_6]$) and PW has the catalytic activity for the reduction of H_2O_2. Therefore, the PDDA–PB film acted as an electron-transfer mediator between the electrode and H_2O_2 [29,31]. It is confirmed that

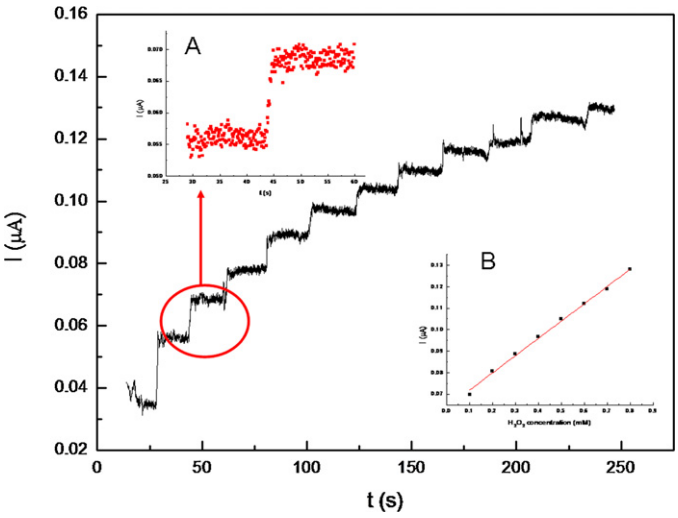

Fig. 7. Current–time amperometric response of $(PAA–graphene/PDDA–PB)_4$ multilayer modified electrode with successive addition of 0.1 mM H_2O_2 into stirring PBS of pH 7.4, 0.1 M KCl solution. Inset A shows the steady-state current response time of the modified electrode to 0.1 mM H_2O_2. Inset B is the calibration curve.

the $(PAA–graphene/PDDA–PB)_4$ multilayer films could be used for determination of H_2O_2 or fabrication of biosensors.

Analytical performance of the $(PAA–graphene/PDDA–PB)_4$ multilayer film electrode in H_2O_2 detection was done. Fig. 7 gave the amperometric responses of the $(PAA–graphene/PDDA–PB)_4$ multilayer film electrode to continual addition of H_2O_2. The cathodic current increased with successive addition of 0.1 mM H_2O_2. It was observed that the $(PAA–graphene/PDDA–PB)_4$ multilayer film electrode responded quickly to the change of H_2O_2 concentration and reached a steady-state signal within 2 s (shown in inset A). This showed advantages in H_2O_2 detection, as compared with some reported H_2O_2 sensors [31,37]. However, as shown in the inset B, the result that the peak currents increased linearly ($R = 0.996$, $n = 8$) from 0.1 mM to 0.8 mM of H_2O_2 was not the most advantageous analytical performance in H_2O_2 detection. This may be due to the less assembled amount of PDDA–PB in the $(PAA–graphene/PDDA–PB)_4$ multilayer film. But, the film thickness and the amount of PDDA–PB could be readily adjusted with the LbL technique for tuning the electroactivity towards H_2O_2 reduction. Experiments on the improvement of its electroactivity towards the reduction of H_2O_2 and on its further application in developing biosensors are in progress and will be reported separately.

4. Conclusions

We have demonstrated a new route to fabricate graphene-based multilayer ultrathin composite films with LbL assembly technique. The growth of the ultrathin film was monitored by UV–vis spectroscopy. Furthermore, based on the synergistic effect of graphene and PB nanoparitcles, the multilayer exhibited catalytic activity toward the reduction of H_2O_2. It could be expected that the electrocatalytic activity of the film could be tailored by simply choosing the number of bilayers, choosing electoactive species, etc. By combining the unique properties of graphene and the versatility of LbL assembly, we expect that this work will stimulate the development of highly efficient electrochemical sensors and advanced biosensing system.

Acknowledgments

This work was financially supported by the National Nature Science Foundation of China (Nos. 21003084, 21271115), Shandong

Province Promotive Research Foundation for Excellent Young and Middle-Aged Scientists (No. BS2010CL023), and the Taishan Scholar Foundation of Shandong Province, China.

References

[1] K.S. Novoselov, A.K. Geim, S.V. Morozov, D. Jiang, Y. Zhang, S.V. Dubonos, I.V. Grigorieva, A.A. Firsov, Electric field effect in atomically thin carbon films, Science 306 (2004) 666–669.
[2] T. Cassagneau, J.H. Fendler, High density rechargeable lithium-ion batteries self-assembled from graphite oxide nanoplatelets and polyelectrolytes, Adv. Mater. 10 (1998) 877–881.
[3] S. Gilje, S. Han, M. Wang, K.L. Wang, R.B. Kaner, A chemical route to graphene for device applications, Nano Lett. 7 (2007) 3394–3398.
[4] F. Schedin, A.K. Geim, S.V. Morozov, E.W. Hill, P. Blake, M.I. Katsnelson, K.S. Novoselov, Detection of individual gas molecules adsorbed on grapheme, Nat. Mater. 6 (2007) 652–655.
[5] J.S. Bunch, A.M. van der Zande, S.S. Verbridge, I.W. Frank, D.M. Tanenbaum, J.M. Parpia, H.G. Craighead, P.L. McEuen, Electromechanical resonators from graphene sheets, Science 315 (2007) 490–493.
[6] M. Zhou, Y.M. Zhai, S.J. Dong, Electrochemical sensing and biosensing platform based on chemically reduced graphene oxide, Anal. Chem. 81 (2009) 5603–5613.
[7] Y. Wang, Y.M. Li, L.H. Tang, J. Lu, J.H. Li, Application of graphene-modified electrode for selective detection of dopamine, Electrochem. Commun. 11 (2009) 889–892.
[8] J. Li, S.J. Guo, Y.M. Zhai, E.K. Wang, Nafion–graphene nanocomposite film as enhanced sensing platform for ultrasensitive determination of cadmium, Electrochem. Commun. 11 (2009) 1085–1088.
[9] Y.X. Fang, S.J. Guo, C.Z. Zhu, Y.M. Zhai, E.K. Wang, Self-assembly of cationic polyelectrolyte-functionalized graphene nanosheets and gold nanoparticles: a two-dimensional heterostructure for hydrogen peroxide sensing, Langmuir 26 (2010) 11277–11282.
[10] C.Z. Zhu, S.J. Guo, Y.M. Zhai, S.J. Dong, Layer-by-layer self-assembly for constructing a graphene/platinum nanoparticle three-dimensional hybrid nanostructure using ionic liquid as a linker, Langmuir 26 (2010) 7614–7618.
[11] C.S. Shan, H.F. Yang, D.X. Han, Q.X. Zhang, A. Ivaska, L. Niu, Water-soluble graphene covalently functionalized by biocompatible poly-L-lysine, Langmuir 25 (2009) 12030–12033.
[12] G.H. Zeng, Y.B. Xing, J. Gao, Z.Q. Wang, X. Zhang, Unconventional layer-by-layer assembly of graphene multilayer films for enzyme-based glucose and maltose biosensing, Langmuir 26 (2010) 15022–15026.
[13] S. Liu, J.F. Ou, Z.P. Li, S.R. Yang, J.Q. Wang, Layer-by-layer assembly and tribological property of multilayer ultrathin films constructed by modified grapheme sheets and polyethyleneimine, Appl. Surf. Sci. 258 (2012) 2231–2236.
[14] A. Rani, K.A. Oh, H. Koo, H.J. Lee, M. Park, Multilayer films of cationic grapheme-polyelectrolytes and anionic graphene-polyelectrolytes fabricated using layer-by-layer self-assembly, Appl. Surf. Sci. 257 (2011) 4982–4989.
[15] S.Y. Wang, D.S. Yu, L.M. Dai, D.W. Chang, J.B. Baek, Polyelectrolyte-functionalized graphene as metal-free electrocatalysts for oxygen reduction, ACS Nano 5 (2011) 6202–6209.
[16] J.F. Shen, Y.Z. Hu, C. Li, C. Qin, M. Shi, M.X. Ye, Layer-by-layer self-assembly of graphene nanoplatelets, Langmuir 25 (2009) 6122–6128.
[17] G. Decher, Fuzzy nanoassemblies: toward layered polymeric multicomposites, Science 277 (1997) 1232–1237.
[18] R.M. Iost, F.N. Crespilho, Layer-by-layer self-assembly and electrochemistry: applications in biosensing and bioelectronics, Biosens. Bioelectron. 31 (2012) 1–10.
[19] Y. Jia, Y. Cui, J.B. Fei, M.C. Du, L.R. Dai, J.B. Li, Y. Yang, Construction and evaluation of hemoglobin-based capsules as blood substitutes, Adv. Funct. Mater. 22 (2012) 1446–1453.
[20] L. Gao, J.B. Fei, J. Zhao, W. Cui, Y. Cui, J.B. Li, pH- and redox-responsive polysaccharide-based microcapsules with autofluorescence for biomedical applications, Chem. Eur. J. 18 (2012) 3185–3192.
[21] J. Zhao, Y. Cui, A.H. Wang, J.B. Fei, Y. Yang, J.B. Li, Side effect reduction of encapsulated hydrocortisone crystals by insulin/alginate shells, Langmuir 27 (2011) 1499–1504.
[22] W. Qi, L. Duan, J.B. Li, Fabrication of glucose-sensitive protein microcapsules and their applications, Soft Matter 7 (2011) 1571–1576.
[23] Y. Jia, J.B. Fei, Y. Cui, Y. Yang, L. Gao, J.B. Li, pH-responsive polysaccharide microcapsules through covalent bonding assembly, Chem. Commun. 47 (2011) 1175–1177.
[24] J. Hong, S.W. Kang, Hydrophobic properties of colloidal films coated with multiwall carbon nanotubes/reduced grapheme oxide multilayers, Colloids Surf., A 374 (2011) 54–57.
[25] W. Qi, L. Duan, X.H. Yan, K.W. Wang, J.B. Fei, Y. Cui, J.B. Li, Triggered release of insulin from glucose-sensitive enzyme multilayer shells, Biomaterials 30 (2009) 2799–2806.
[26] S.W. Lee, B.S. Kim, S. Chen, Y. Shao-Horn, P.T. Hammond, Layer-by-layer assembly of all carbon nanotube ultrathin films for electrochemical applications, J. Am. Chem. Soc. 131 (2009) 671–679.
[27] S.H. Lee, D.H. Lee, W.J. Lee, S.O. Kim, Tailored assembly of carbon nanotubes and graphene, Adv. Funct. Mater. 21 (2011) 1338–1354.
[28] Q. He, Y. Cui, J.B. Li, Molecular assembly and application of biomimetic microcapsules, Chem. Soc. Rev. 38 (2009) 2292–2303.
[29] L. Wang, S.J. Guo, X.G. Hu, S.J. Dong, Layer-by-layer assembly of carbon nanotubes and Prussian blue nanoparticles: a potential tool for biosensing devices, Colloids Surf., A 317 (2008) 394–399.
[30] F.H. Li, C.S. Shan, X.Y. Bu, Y.F. Shen, G.F. Yang, L. Niu, Fabrication and electrochemical characterization of electrostatic assembly of polyelectrolyte-functionalized ionic liquid and Prussian blue ultrathin films, J. Electroanal. Chem. 616 (2008) 1–6.
[31] F.L. Qu, A.W. Shi, M.H. Yang, J.H. Jiang, G.L. Shen, R.Q. Yu, Preparation and characterization of prussian blue nanowire array and bioapplication for glucose biosensing, Anal. Chim. Acta 605 (2007) 28–33.
[32] T. Uemura, M. Ohba, S. Kitagawa, Size and surface effects of prussian blue nanoparticles protected by organic polymers, Inorg. Chem. 43 (2004) 7339–7345.
[33] W.S. Hummers, R.E. Offeman, Preparation of graphitic oxide, J. Am. Chem. Soc. 80 (1958) 1339.
[34] A.A. Karyakin, Prussian blue and its analogues: electrochemistry and analytical applications, Electroanalysis 13 (2001) 813–819.
[35] A.A. Karyakin, E.A. Puganova, I.A. Budashov, I.N. Kurochkin, E.E. Karyakina, V.A. Levchenko, V.N. Matveyenko, S.D. Varfolomeyev, Prussian blue based nanoelectrode arrays for H_2O_2 detection, Anal. Chem. 76 (2004) 474–478.
[36] I.L. de Mattos, L. Gorton, T. Ruzgas, A.A. Karyakin, Sensor for hydrogen peroxide based on Prussian Blue modified electrode. Improvement of the operational stability, Anal. Sci. 16 (2000) 795–798.
[37] A. Salimi, A. Noorbakhsh, H. Mamkhezri, R. Ghavami, Electrocatalytic reduction of H_2O_2 and oxygen on the surface of thionin incorporated onto MWCNTs modified glassy carbon electrode: application to glucose detection, Electroanalysis 19 (2007) 1100–1108.